

Current Trend of Carbon Emissions from Wildfires in Siberia

Evgenii Ponomarev ^{1,2,*} , Nikita Yakimov ^{1,2}, Tatiana Ponomareva ^{2,3}, Oleg Yakubailik ^{1,2} and Susan G. Conard ⁴

¹ Federal Research Center “Krasnoyarsk Science Center, Siberian Branch, Russian Academy of Sciences”, Krasnoyarsk 660036, Russia; nyakimov96@mail.ru (N.Y.); oleg@icm.krasn.ru (O.Y.)

² Department of Ecology and Environment, Siberian Federal University, Krasnoyarsk 660041, Russia; bashkova_t@mail.ru

³ V.N. Sukachev Institute of Forest, Siberian Branch, Russian Academy of Sciences, Krasnoyarsk 660036, Russia

⁴ Department of Geography and Geoinformation Science, Affiliate Faculty, George Mason University, Fairfax, VA 22030, USA; sgconard@aol.com

* Correspondence: evg@ksc.krasn.ru; Tel.: +73-91-249-40-92

Abstract: Smoke from wildfires in Siberia often affects air quality over vast territories of the Northern hemisphere during the summer. Increasing fire emissions also affect regional and global carbon balance. To estimate annual carbon emissions from wildfires in Siberia from 2002–2020, we categorized levels of fire intensity for individual active fire pixels based on fire radiative power data from the standard MODIS product (MOD14/MYD14). For the last two decades, estimated annual direct carbon emissions from wildfires varied greatly, ranging from 20–220 Tg C per year. Sporadic maxima were observed in 2003 (>150 Tg C/year), in 2012 (>220 Tg C/year), in 2019 (~180 Tg C/year). However, the 2020 fire season was extraordinary in terms of fire emissions (~350 Tg C/year). The estimated average annual level of fire emissions was 80 ± 20 Tg C/year when extreme years were excluded from the analysis. For the next decade the average level of fire emissions might increase to 250 ± 30 Tg C/year for extreme fire seasons, and to 110 ± 20 Tg C/year for moderate fire seasons. However, under the extreme IPCC RPC 8.5 scenario for Siberia, wildfire emissions might increase to 1200–1500 Tg C/year by 2050 if there were no significant changes in patterns of vegetation distribution and fuel loadings.

Keywords: wildfire; Siberia; carbon emissions; remote sensing



Citation: Ponomarev, E.; Yakimov, N.; Ponomareva, T.; Yakubailik, O.; Conard, S.G. Current Trend of Carbon Emissions from Wildfires in Siberia. *Atmosphere* **2021**, *12*, 559. <https://doi.org/10.3390/atmos12050559>

Academic Editors: Anthony R. Lupo and Chris G. Tzanis

Received: 31 March 2021

Accepted: 23 April 2021

Published: 26 April 2021

Publisher's Note: MDPI stays neutral with regard to jurisdictional claims in published maps and institutional affiliations.



Copyright: © 2021 by the authors. Licensee MDPI, Basel, Switzerland. This article is an open access article distributed under the terms and conditions of the Creative Commons Attribution (CC BY) license (<https://creativecommons.org/licenses/by/4.0/>).

1. Introduction

Carbon emissions from wildfires are a significant factor affecting air quality over large areas of the Northern hemisphere during the fire season in the boreal forests and tundra of Siberia (May–August) [1,2]. Siberian wildfires are responsible for most of the annual burned area in Russia (70% of fire events and up to 90% of the total burned area) [3,4]. Every year, about 5–20 MHa of forests are affected by wildfires there [4]. Smoke from these fires can be transported thousands of kilometers from the zone of mass wildfires depending on atmospheric circulation patterns and on current meteorological conditions [5]. Wildfire emissions frequently affect air quality in the main cities of central and southern Siberia (Novosibirsk, Krasnoyarsk, Yakutsk, and Irkutsk etc.). In some years, the smoke from Siberia has been transported to European Russia (in 2012, 2016), or to the Russian Far East (in 2003), as well as to the Arctic (in 2019) [5–7] and North America [8,9]. Transboundary transfers of fire emissions to neighboring countries have also been observed [10].

For Siberia, the range of carbon emissions and accuracy of burned area estimates have been studied for several decades [1,2,11–14]. According to Conard et al. [1], estimated emissions for Russian boreal forests in 1998 were from 135 to 190 Tg C. Soja et al. [11] calculated that potential annual fire emissions between 1998 and 2002 could range from 116 to over 500 Tg C/year depending on annual burned area and fuel consumption rates.

These estimates [1,2,11–14] should be considered as first approximations since the referenced estimates are based on the burned area and do not explicitly consider variations

in burning intensity within each fire event. For precise estimates, it is necessary to consider spatial and temporal differences in fire intensity and fuel consumption. This would require emissions to be calculated for every part of a burned area based on differences in burning characteristics. Using satellite data, it is possible to obtain more accurate estimates of active burning zones and burned areas [14,15] as well as of the intensity of combustion and various emission components [16–18]. Wooster et al. [16] showed that the biomass combustion rate is linearly related to fire radiative power (FRP, MW/km²) in experimental fires. This is the basis for the standard products MOD14/MYD14 from Terra/Aqua/MODIS (<https://ladsweb.modaps.eosdis.nasa.gov/>, accessed on 25 March 2021) [17,18]. Improved accuracy of biomass combustion and carbon emissions estimates requires accounting for burning characteristics of individual fire polygons to reflect spatial variability in fire behavior and fuel consumption. Extreme estimates [11] of emissions for Siberia assume high-severity fire across the landscape, which is unlikely except under the most severe local or regional conditions. Other recent estimates for Russia suggest long-term average values of 120–240 Tg C/year [19,20]. Clearly more accurate estimates of fire emissions are important for a full understanding of the impact of wildland fires on the atmosphere and on terrestrial carbon budget.

The aim of this study was to estimate variation and trends of carbon emissions from wildfires over the past two decades in the Siberian forest, forest-steppe, and tundra by incorporating FRP data from individual active zones (active fire pixels) within each fire polygon.

2. Materials and Methods

2.1. Study Area

Siberia covers about 9.7×10^6 km² between 50–75° N and 60–150° E (Figure 1). This is about 56.64% of the area of Russia. The area of Siberian forests is estimated at 6.0×10^6 km². About 70% of Russian forests (including sparse larch stands) are in Siberia [4]. The major forest types in Siberia are dominated by larch (*Larix sibirica*, *L. gmelinii*, and *L. cajanderi*), Scots pine (*Pinus sylvestris*), dark coniferous forest (*Pinus sibirica*, *Abies sibirica*, *Picea obovata*), Siberian dwarf pine (*Pinus pumila*), birch (*Betula* spp.), and aspen (*Populus tremula*) species. Based on data from Vega-service (Service of the Russian Academy of Sciences' Space Research Institute, IKI, Moscow, <http://pro-vega.ru/maps/>, accessed on 25 March 2021), forests dominated by larch cover an area of 2.7 – 3.0×10^6 km²; the area of Scots pine stands is 1.0×10^6 km²; dark coniferous stands occupy 0.75×10^6 km²; and mixed forest covers about 0.77×10^6 km². *Pinus pumila* covers about 0.25×10^6 km² at the interface between taiga and tundra [21]. We evaluated fire activity in these forest areas and tundra using GIS geospatial calculations for Azimuthal Equidistant projection and Sphere geoid (WGS_1984).

2.2. Data on Wildfires

We used the V.N. Sukachev Institute of Forest (Krasnoyarsk, Russia) wildfire database for Siberia created using remote sensing data obtained by our receiving station in Krasnoyarsk in 2002–2020 (Figure 2).

The information on wildfires was stored as a geographic information system (GIS) polygon layer, with attributive data on coordinates, dates, fire shape, and its daily dynamics, as well as on area burned (Figure 3) [22]. The processing chain for the initial MODIS data was based on the approach of Giglio et al. [23]. Our algorithm differs mainly in its approach for aggregating fire detections (fire pixels) into fire polygons and subsequently using a correction procedure for precise estimates of the burned area [22]. For this paper, we considered all vegetation fires detected by remote sensing over the territory of Siberia for 2002–2020 (Figure 2). Active fire products of MODIS data for fire radiative power (MOD14/MYD14) were acquired from the Level-1 and Atmosphere Archive and Distribution System (LAADS) Distributed Active Archive Center (DAAC) website (<https://ladsweb.modaps.eosdis.nasa.gov/>, accessed on 25 March 2021).

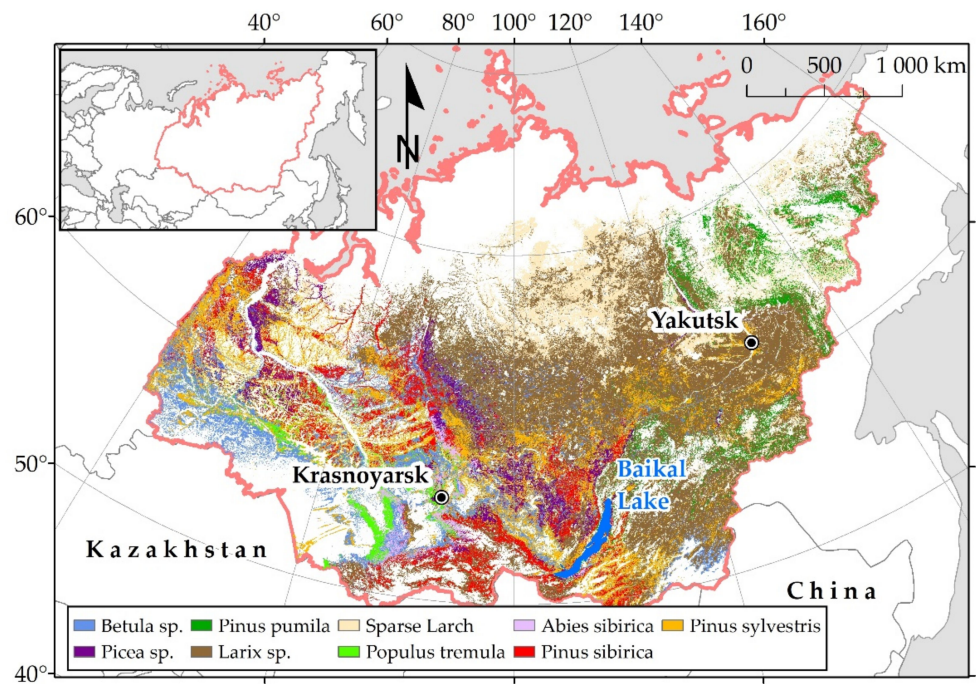


Figure 1. Territory of Siberia. Main Siberian forest types (based on <http://pro-vega.ru/maps/>, accessed on 25 March 2021) [21]. Forest types range from “sparse” (crown closure <20%) to “closed” (>80% crown closure) tree stands.

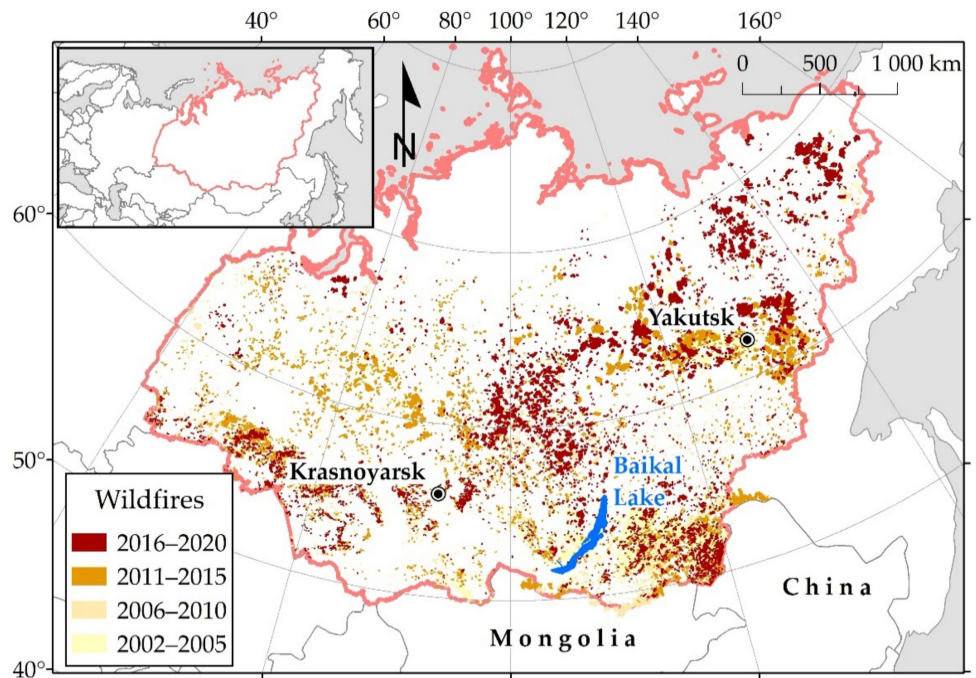


Figure 2. Spatial distribution of wildfires in 2002–2020. Only burned areas >2500 ha are shown.

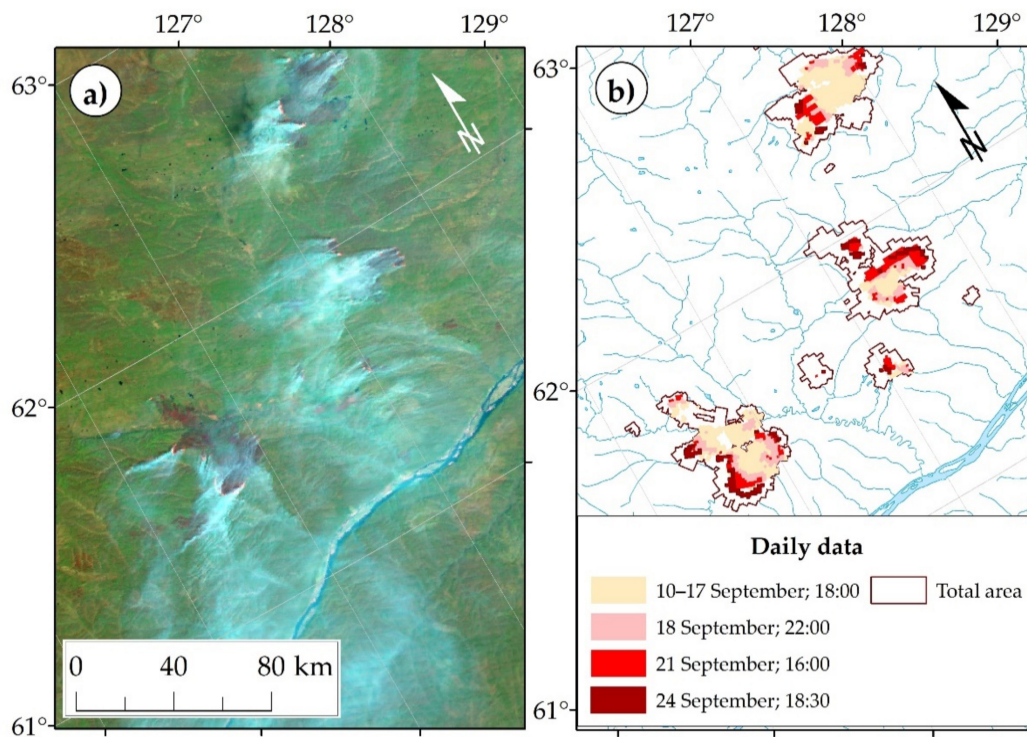


Figure 3. Active burning in Siberia in September of 2020: active wildfires and smoke plumes on Terra/MODIS imagery on 24 September (a) and daily records from wildfire database of active burning detected from 10–24 September 2020 (b).

2.3. Classification of Wildfire Polygons in Terms of FRP

For every active fire pixel within a wildfire polygon (Figure 3), we calculated statistics for mean fire radiative power (FRP_{mean}) and standard deviation (SD). Next, we classified all fire pixels from the database into three categories of FRP: fire pixels of low FRP ($FRP < FRP_{mean} - \sigma$), fire pixels of medium FRP ($FRP_{mean} - \sigma < FRP < FRP_{mean} + \sigma$), and fire pixels of high FRP ($FRP > FRP_{mean} + \sigma$) [24]. Thus, we distinguished areas of wildfire polygons (A) corresponding to parts of the burned area with low, medium, and high FRP ($A_i(FRP_i)$), which are determined by the amount and rate of combustion of biomass according to [16].

$$A = \sum_i A_i(FRP_i) \quad (1)$$

Early numerical simulation indicated a tendency toward an increase in the FRP fraction with an increase in the flame-front propagation rate [24]. An increase in the specific combustion rate of fuel (kg/m^2s) doubles the range of recorded FRP values with a shift of the maximum to 200 MW per pixel, taking into account the subpixel value of the active combustion area. We quantified the dependence of FRP on the fire front rate of spread and the fuel load in the active combustion zone (kg/m^2) [24]. Assuming a linear relationship between FRP and consumption, we defined a range of the values of the fraction of biomass consumed during wildfire events.

2.4. Estimation of Fire Emissions of Carbon

The amount of direct carbon emissions was calculated using the Seiler–Crutzen ratio [25]:

$$C = A \times B \times CE \times \beta \quad (2)$$

where A is area burned by fire (m^2); B is biomass density or pre-fire forest fuel load (kg/m^2); CE is the carbon fraction of the biomass (g/kg); β is the fraction of biomass consumed during wildfire events.

The burned area (A , m^2) was the sum of the burned areas having various categories of intensity using (1). Thus, we calculated the sum of burned areas for each intensity class and fuel type and then estimated the consumption separately for each intensity/fuel type combination. We have calculated the amount of burned biomass using coefficients derived for each of these combinations (2).

We linked every record from the wildfire database to dominant vegetation types available for Siberia from the Vega-service (<http://pro-vega.ru/maps/>, accessed on 25 March 2021) [21] using the GIS procedure for the intersection of vector layers. Forest type characteristics and pre-fire fuel loads were summarized from field data [1,2,11–13,26,27].

Pre-fire fuel loads ($B = 1.38$ – 5.4 kg/m^2) were obtained from published data [12,27,28]. We used generalized data on surface fuels in forests with a prevalence of larch, pine, dark coniferous, and deciduous stands as the input parameter.

We determined values of β for the three FRP categories based on empirical estimates of fuel consumption during wildfires of various intensities: β was selected as 0.35–0.40 for low FRP, 0.40–0.45 for medium FRP, and 0.45–0.60 for high FRP. We considered also various empirical estimates [1,2,11,12] of forest fuels combusted during wildfires of various intensities: 0.11–0.97 kg/m^2 , 0.86–2.15 kg/m^2 , and 2.25–5.36 kg/m^2 , respectively, for low-, medium-, and high-intensity fires.

In the resulting series of emissions for 2002–2020, we singled out separately years with sporadic maxima, years of minimal emissions, and years of mean \pm SD values.

As additional criteria, to separate data of “moderate” and “low” season emissions, we analyzed annual emissions compare to the average values for 2002–2011 (59.5 Tg C/year) and 2012–2020 (115.7 Tg C/year). If emissions were lower than one confidence interval than the average value, the year was classified as the season of minimal emissions.

We derived exponential regression relationships for three types of fire seasons: (1) for the case of a moderate scenario of burning in Siberia, (2) for the case of low burning scenario, and (3) for the case of extreme burning. The resulting equations were used to evaluate trends, calculate average levels of fire emissions and extrapolate the potential increase in emissions by 2050.

3. Results

3.1. Fire Statistics

From 2002–2020 the total number of wildfires in Siberia was $> 3 \times 10^5$. We have summarized wildfire statistics for 5-year periods (burned area data were available for 2001, but not FRP data). These intervals illustrate the dynamics of wildfires in Siberia over the past two decades (Figure 2, Table 1). While the number of wildfires did not show a trend over this period, the average annual burned areas in the 2011–2020 decade were more than double those from 2001–2010, suggesting a substantial increase in average annual burned areas after 2010. Table 1 contains data on all fires in the database, including forest, tundra, and steppe vegetation zones.

Table 1. Wildfire statistics for Siberia for 5-year intervals (mean value \pm SD, $p < 0.05$).

Intervals	Number of Wildfires, $\times 1000$	Burned Area, MHa
2001–2005	11.18 \pm 5.07	6.32 \pm 3.83
2006–2010	19.72 \pm 3.56	7.56 \pm 2.12
2011–2015	17.30 \pm 4.30	15.40 \pm 4.09
2016–2020	13.72 \pm 2.44	16.06 \pm 6.84
20-year average	15.48 \pm 2.33	11.34 \pm 2.88

We also evaluated the distribution of fires in Siberia by vegetation cover types for forest and tundra zones. Dark coniferous forest includes spruce, fir, Siberian pine; deciduous forests include birch and aspen; and the category of “other” includes various mixed vegetation types and northern tundra vegetation (Table 2). Table 2 contains data

(percentage) on forest and tundra fires only, and the total number and total burned area did not include steppe fire statistics. We used relative fire characteristics to compare the fire regimes in different forest types. Relative burned area (RBA) is the percent of a vegetation type burned annually, and the relative fire frequency (RFF) is the number of annual fire events per 10^6 ha of forest stands of different species.

Table 2. The percentage of total (forest and tundra) fire occurrences and burned area and the relative burned area (RBA, %) and the relative frequency of fires (RFF, events per 10^6 ha of forest) by vegetation cover types. Data averaged for 2002–2020.

Dominant Tree Stand	Area of Tree Stands, 10^6 ha	Number of Wildfires, % of Total	RFF, per 10^6 ha Per Year	Burned Area, % of Total	RBA, % of Burned Annually
Larch (<i>Larix sibirica</i> , <i>L. dahurica</i> , <i>L. cajanderi</i>)	~300	43.1	8.7	60.0	1.10
Scots pine (<i>Pinus sylvestris</i>)	95	26.0	16.7	16.9	0.97
Deciduous (<i>Populus tremula</i> and <i>Betula</i> spp.)	77	20.6	16.4	13.2	0.99
Dark coniferous stands (<i>Pinus sibirica</i> , <i>Abies sibirica</i> , <i>Picea obovata</i>)	75	7.0	5.6	6.4	0.49
Interface between taiga and tundra (<i>Pinus pumila</i>)	25	0.5	1.2	3.2	0.73
Other types/Tundra	~180	2.8	1.0	0.3	0.01

Over half of the burned area was in larch-dominated stands, followed by Scots pine stands, while the lowest percentage of the total burned area was in dark coniferous stands, within the interface between taiga and tundra covered by *Pinus pumila*, and in tundra (Table 2). The larch and Scots pine forests have mixed fire regimes with relatively frequent low to moderate severity surface fires and occasional severe fires where overstory trees experience high mortality. Dark coniferous forests mostly burn in infrequent high-severity stand replacement fire.

Almost 90% of all burned areas in the Siberian forest and tundra regions are in forests dominated by larch, pine, and deciduous tree species. These fires determine the main contributors to carbon emissions, the contribution of fires in dark coniferous forests is significantly lower, and the share of emissions from fires in the tundra (above 67 + N) is still negligible as they comprise <1% of total burned area.

3.2. Ratio of Fire Intensity Areas

The total number of preprocessed fire pixels was $\sim 2.23 \times 10^6$, which includes data on 3.1×10^5 wildfires in Siberia recorded for 2002–2020.

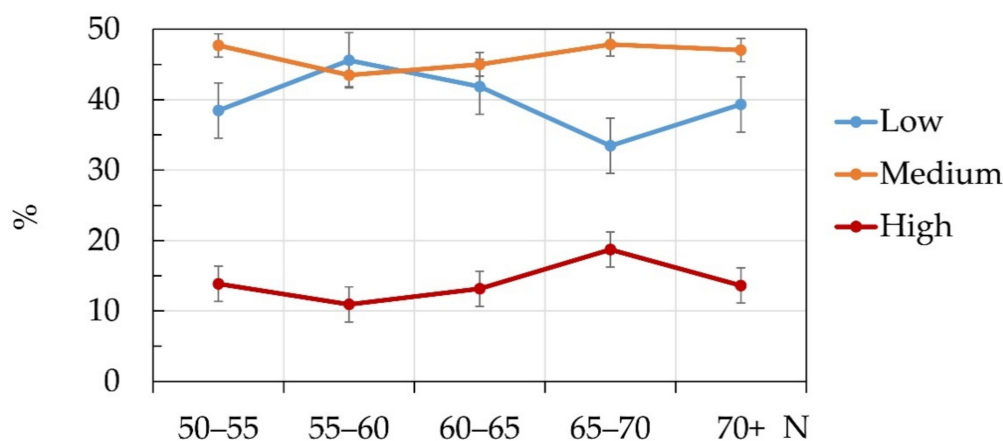
FRP for most of the fire pixels (up to 88% of the total) was below 50 MW/km². The mean value of FRP was 37.4 MW/km² (at the 95% confidence level), and SD was 17.1 MW/km². We defined two threshold values to separate fire pixels by FRP/intensity categories, namely 20.3 MW/km² and 54.5 MW/km² [24,29].

We classified the proportion of low, medium, and high-intensity fire areas according to the FRP categories. Additionally, we assessed the change in the ratio of these categories across the latitudinal gradient, which is accompanied by a change in the prevailing types of vegetation cover (Table 3).

Table 3. Percent of low-, medium- and high-intensity fire areas on a latitudinal gradient and associated dominant vegetation types.

Latitude Range, N	% of Total Burned Area			Dominant Vegetation
	Low	Medium	High	
70+	39.3	47.1	13.6	Tundra and bog vegetation
65–70	33.5	47.8	18.7	Sparse larch, <i>Pinus pumila</i>
60–65	41.8	45.0	13.2	Larch, Scots pine, mixed forests
55–60	45.6	43.5	10.9	Scots pine, deciduous, dark coniferous
50–55	38.5	47.7	13.8	Steppe vegetation, mountain forests, dark coniferous

On average, the ratio of low-, medium- and high-intensity fires in Siberia was 39.7 ± 3.9 , 46.2 ± 1.7 , and $14.1 \pm 2.5\%$, respectively. Variation in the ratio of fires of different intensities on a latitudinal gradient was primarily related to the redistribution of low and high-intensity fires (Figure 4).

**Figure 4.** Ratio of fires of low, medium, and high intensities on a latitudinal gradient 50° – 70° + N.

3.3. Direct Carbon Emissions

Our estimate of carbon emissions from wildfires in Siberian forest and tundra was 80 ± 20 Tg C/year. Between 2002 and 2020, direct fire emissions varied from the minimum values of 20–40 Tg C/year (under conditions of low fire danger of 2004, 2005, 2007, 2009, 2010) to maxima of ~350 Tg C/year (in the extraordinary season of 2020). For the last two decades, maximum emissions were estimated for the extreme fire seasons of 2003 (>150 Tg C/year), in 2012 (>220 Tg C/year), in 2019 (~180 Tg C/year). However, the 2020 fire season was extraordinary in terms of fire emissions, which was four times the average value in the 2011–2020 decade (Figure 5).

On average, over 50 percent of emissions were estimated to come from fires in larch forests and 13–14 percent from pine forests. Other forests and tundra combined produced only 7–10 percent of annual emissions (Table 4).

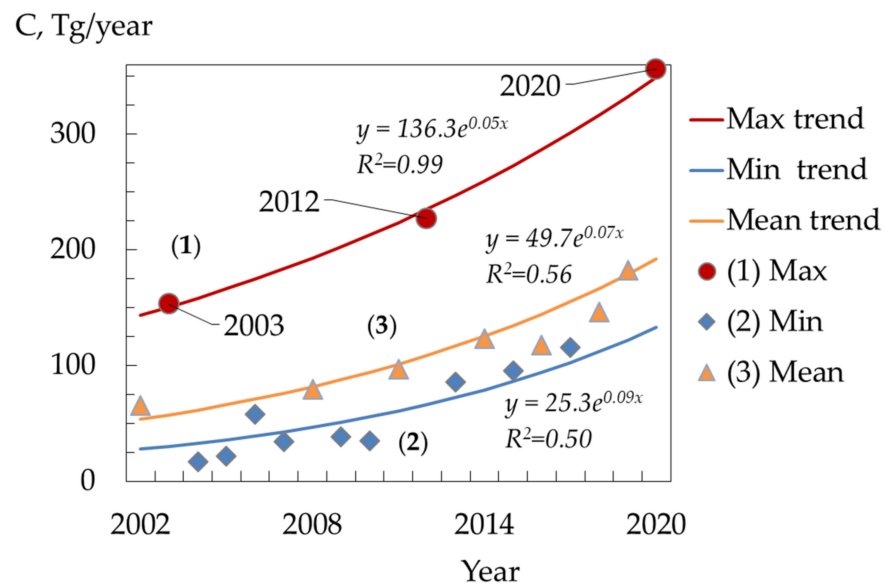


Figure 5. Annual data on wildfire emissions from fires in Siberia for 2002–2020 and current trends of emission: (1) estimated values and trend for sporadic maximum emissions, (2) estimated values and trend for minimum emissions, and (3) estimated values and trend for emission values without including extremes.

Table 4. Estimates of carbon emissions per year (Tg C/year) and per area of forest (Mg C/ha) by vegetation cover types (range for moderate and extreme fire seasons).

Dominant Vegetation	Tg C/year	Mg C/ha	% of Annual Emission (Min–Max)
Larch	43.0–52.0	15.5–18.8	51.6–62.4
Pine	11.0–12.0	16.7–18.0	13.2–14.2
Deciduous/mixed	3.8–5.0	13.7–17.5	4.5–5.7
Dark coniferous	1.9–3.1	12.7–20.4	2.3–3.7
Tundra and bog vegetation (of 70 + N)	0.2–1.0 *	NA	0.2–0.8

* Data for 2020 (3.7 Tg C/year) were excluded because it was the only season in the resulting series with more than 5 times of the average (0.58 ± 0.35) emissions for this sub-region of 70 + N. Even in that year, emissions from tundra and peat bog sites were only a little over 1.05 percent of total fire emissions.

To identify the current trends in carbon emissions from fires in Siberia, we considered separately the extremes only: (1) seasons of sporadic maximum emissions, (2) seasons with minimum emissions, as well as (3) seasons with moderate emissions. We obtained separate regression relationships for these three types of fire seasons (Figure 5).

We used the exponential function $C = A_0 \exp(bY_{r_i})$, where C is emissions, Y_{r_i} is year number ($i = 1 \dots 19$) in the 2002–2000 period, $A_0 = 25, 50,$ and 136 were the initial emission levels for scenarios of minimum, average and maximum burning in Siberia, respectively. The coefficient b was 0.087, 0.07, and 0.05 for scenarios of minimum, average and maximum burning as well and $R^2 = 0.50$ – 0.99 .

Extrapolating from these regressions, for the next several decades, the average level of fire emissions might increase to 250 ± 30 Tg C/year for the case of extreme climate and fire activity, to 65 ± 15 Tg C/year in the case of low fire danger seasons, and to 110 ± 20 Tg C/year in the case of moderate fire seasons. Based on these equations, we also projected that potential emissions from fires in Siberia might range from 1200–1500 Tg C/year by 2050, which corresponds to a rather extreme scenario of IPCC (RPC 8.5) for Siberia [30].

4. Discussion

4.1. Burning in Forests of Siberia

The annual burned area (Table 1) strongly determined the year-to-year variation in estimated carbon emissions (Figure 5) from fires in Siberia [1,14,28]. The current trend of increasing burned area is a significant factor in the carbon emission trend as well. In the context of climate change, prolonged summer droughts, and redistribution of precipitation, fires can develop over large areas [31,32], including a shift to higher fire activity at the northern border of the forest and into the tundra [4,33,34].

Vegetation types of Siberia vary widely in their fire regimes (frequency and severity of fires) as a function of local or regional climate, vegetation composition, and fuel structure. References provided in the Methods section address these patterns. The most widely distributed forest types in Siberia are dominated by larch, including sparse larch stands. Forests dominated by larch cover an area of $270\text{--}300 \times 10^6$ ha. This is almost 50% of the total forest area in Siberia. In addition, many larch forests have a fire regime dominated by frequent low severity surface fires. Thus, it is not surprising that >43% of the Table observed fire events and 60% of the total burned area were in larch forests.

Relative characteristics such as the relative burned area (RBA, % of a forest type burned annually) and the relative frequency of fires (RFF, events per 10^6 ha of forest) (Table 2) permit comparison of area burned or the number of fires in stands dominated by different tree species in relation to their total area coverage. RBA is highest in forests dominated by larch (1.10), deciduous tree stands (0.99), and Scots pine (0.97). While the number of fires is highest in deciduous (16.4 events per 10^6 ha) and pine (16.7 events per 10^6 ha) forests of Siberia, the average fire size is less than in larch forest. Thus, the larch forests of Siberia are characterized by higher burned areas than other forest types.

Wildfires are the most important driver of forest dynamics in Siberia [4] and throughout the boreal zone [5,28,35], and fire impacts vary significantly in different forest types, which is important in terms of fire emissions. Based on long-term data on wildfires, more than 93% of all burned areas are in forests with a predominance of larch, pine, and deciduous species of Siberia. These fires determine the main contributors to carbon emissions. Fires in the larch forests of the East Siberian plateau taiga region ($60\text{--}70^\circ$ N, $100\text{--}140^\circ$ E) provided >60% of direct fire emission. The contribution of fires in dark coniferous forests was significantly lower (up to 3.7% of total), and the share of emissions from fires in the tundra (above 67° N) is still negligible (<1% of total). This assessment based on satellite data is similar to published data on the Asian part of Russia (east of the Urals) for burned areas in larch forests (up to 50% of the total), dark coniferous (about 5%), light coniferous, and deciduous (18% and 19%, respectively) by other authors for different years and shorter time periods [11,28].

To improve the accuracy of estimates, we categorized levels of fire intensity for individual active fire pixels based on FRP methodic. Previously, the data on FRP for fires in Siberia was verified experimentally. We evaluated FRP in relation to direct ground-based field measurements of emissions from large-scale wildfires in the Yenisei middle taiga subzone of Siberia in 2012 [7]. The relative contribution of emissions from these large-scale wildfires in 2012 to the background concentration of carbon gases (CO_2 , CH_4 , CO) in the atmospheric boundary layer was directly measured at a single location, the 300-m ZOTTO tall tower (the Zotino Tall Tower Observatory, <https://www.zottoproject.org/>, accessed on 25 March 2021).

We calculate that the combustion efficiency CE, which indirectly defines fire intensity, correlated ($R^2 = 0.49$) with data on FRP for large-scale wildfires. The major (up to 70%) contribution of the emission of carbon gases from wildfires occurred during the flaming phase of combustion, and the rest (~30%) was emitted during smoldering of organic matter, which was characterized by lower FRP values [7].

On average, we estimated the ratio of low-, medium- and high-intensity fires in Siberia as 39.7 ± 3.9 , 46.2 ± 1.7 , and $14.1 \pm 2.5\%$, respectively. Differences in the relative importance of fires of different intensities across a latitudinal gradient were determined

primarily by the relative proportions of low and high-intensity fires. The proportion of medium intensity fires did not change significantly with latitude.

Previously, for 2002–2016 we obtained ratio of burned area of low-, moderate-, and high-intensity fires in Siberia as $47.0 \pm 13.6\%$, $42.5 \pm 10.5\%$, and $10.5 \pm 6.9\%$ [24,36]. In addition, in previous studies, empirical data indicated that the burned areas corresponded to 22%, 38.5%, and 38.5% for low-, medium-, and high-intensity fires, respectively [11], using different methods for characterizing and classifying fire intensity. By a similar method, using FRP statistics we estimated that high-intensity crown fires comprised 8.5% of the annual burned forest area in Siberia [36].

The data presented here (Table 1) show that the average annual burned areas for the past 10 years were about 2.3 times those for the previous 10 years.

For the 1990–2014 period, the number of wildfire events and annual total burned areas were positively correlated ($r \sim 0.6$) with temperature anomalies during the fire season [37]. The precipitation anomalies and standardized precipitation evapotranspiration index (SPEI) were negatively correlated with the number of fires ($r = -0.4$) and burned area (-0.55) [37]. There were also significant correlations ($R^2 \sim 0.63$ – 0.70 , $p < 0.05$) between seasonal variation in fire occurrence in 1996–2016 and the hydrothermal coefficient (HTC, see [38] for details) for the Siberian sub-regions [38]. Thus, we suggest that the combination of higher spring and summer air temperatures and lower precipitation are the most likely causes of increased annual burned area in Siberia since 2010.

In addition, we used the most accurate data available on the areas of fires, linking the fire database to recent data on vegetation cover. Coefficients for the Seiler–Crutzen ratio (2) were taken from published results of experimental fires studied in various forest stands in Siberia [1,2,11–13,26,27]. In addition, we incorporated measurements of combustion intensities for each detected active zone (active fire pixel) of fire (based on FRP). This approach minimized the uncertainty in the determination of coefficients for Equation (2). Assuming a linear relationship between FRP and consumption, we defined a range of the values of the fraction of biomass consumed during each wildfire event. This assumption was based on results described by Wooster et al., 2005 [16], Ichoku, Kaufman, 2005 [17], and Ponomarev et al., 2019 [24]. We believe that this approach leads to more accurate estimates of fire emissions and has the potential to improve future emission forecasting.

4.2. Carbon Emissions

Total carbon emissions from wildfires of forests and tundra varied considerably from year to year, with the lowest emissions of 20–40 Tg C/year and the highest emissions occurring during 2003 (>150 Tg C), 2012 (>220 Tg C), 2019 (~180 Tg C), and 2020 (~350 Tg C) and a mean of 80 ± 20 Tg C/year between 2002 and 2020.

Emissions that are below average were typical for seasons with low fire activity, such as 2004, 2005, 2007, 2009, 2010. The highest emission values occurred in seasons where there were massive fires in the boreal forest zone of Siberia. There is no active fire suppression in the northern part of this zone, so fires can continue to burn for several weeks resulting in large-scale wildfire events.

Over the past two decades, the season of 2020 was extraordinary in terms of fire emissions (~350 Tg C/year). Unusually high spring temperatures in 2020 set the scene for a potentially severe fire season, especially in areas where these extreme temperatures persisted throughout the summer. Burned area data show that there was an unusual amount of fire activity in the 2020 fire season in northern Siberia (north of 65 degrees). This fire activity was associated with severe spring and summer drought that led to extreme fire behavior and long-duration fires [33,39,40]. Thus, according to our estimates, the emissions in the tundra zone in 2020 were four times higher (3.7 Tg C/year) than the average statistical value for 20 years (0.2–1.0 Tg C/year).

According to our approximation for the next decade, the average level of fire emissions might increase to 250 ± 30 Tg C/year in extreme fire seasons and to 110 ± 20 Tg C/year in moderate fire seasons.

There are few publications that provide quantitative estimates of fire emissions in Siberia. This is due to the large uncertainty of the parameters in calculations of this kind. There have been few direct measurements of emissions from fires in Siberia. Most papers contain expert review assessments [5,10,14,19] or data on measurements carried out for limited experimental fires [2,12]. A number of articles with estimates on emissions for certain periods are presented for comparison in our work [1,11].

Our estimates on fire emissions are in the range of previous assessments for Siberian fires, which were from 116 Tg C/year in 1999 up to >500 Tg C/year in 2002, estimated by Soja et al. (2004) [11] and 135 to 190 Tg C for 1998, estimated by Conard et al. [1].

Our estimates of annual fire emissions are for the boreal forests and tundra of Siberia. The level of emissions can be compared with the data for the boreal forests of Alaska and Canada. For 2002–2006 the average of 80 Tg C/year was estimated for Alaska [41]. Veraverbeke et al., 2015 [42] estimated that average annual emissions from forest fires in Alaska in 2001–2012 were between 17 and 69 Tg C/year, while maxima were recorded up to >100 Tg C/year.

Amiro et al. (2001) [43] estimated that direct fire emissions from Canadian forest fires were 27 ± 6 Tg C/year, while individual years ranged from 3 to 115 Tg C/year in 1959–1999. The estimated average fire-caused direct carbon emissions for Canada were up to 57 Tg C/year in 1990–2012 [44]. As with Siberia, these estimates can vary considerably depending on study methods and assumptions. It is also important to note that none of these papers include data later than 2012.

The distribution of fire emissions at a qualitative level can also be obtained based on remote sensing data. One of the most effective tools for analyzing the spread of fire smoke over long distances is the OMPS Aerosol Index [45]. The data recorded by the OMPS/Suomi NPP (the Suomi National Polar-orbiting Partnership) instrument (<https://worldview.earthdata.nasa.gov/>, accessed on 13 April 2021) shows smoke plumes transported thousands of kilometers from active fires in Siberia (Figure 6). These materials are important for understanding the propagation of fire emissions. However, quantitative calibration should be provided, which is only possible when processing data on each individual fire event.

Increases in the annual burned area between 1996 in larch forests of central Siberia have been correlated with both temperatures and drought [46]. Thus, under conditions of increased air temperature [37,40], we expect a correlation between fire emissions and climate change. Previously [6] regression models were used for forecasting emissions under two IPCC climate scenarios, based on fire emissions and summer temperatures in Siberia for 2002–2016 for RCP2.6 (average air temperature increase of 0.3–1.7 °C); and for the “harsh” RCP8.5 scenario (temperature increase of 2.6–4.8 °C) [30]. In this case, fire emissions up to 2000 Tg C/year were projected for the RCP 8.5 scenario [6]. In the current paper, we project a range of emissions from 1200–1500 Tg C/year by 2050, which is similar to the results based on the IPCC RCP 8.5 scenario for Siberia. There is little doubt that the rapidly warming climate in Siberia will lead to continued increasing fire activity over the next several decades.

This is a strong indication that we are already observing the effects of extreme climate warming on fire regimes in Siberia. Such large increases in burned areas are the primary reason for increasing carbon emissions from wildfires over the past two decades. We expect these increases to continue into at least the next several decades, although potential future changes in vegetation and fuels may also affect the trajectory [47,48].

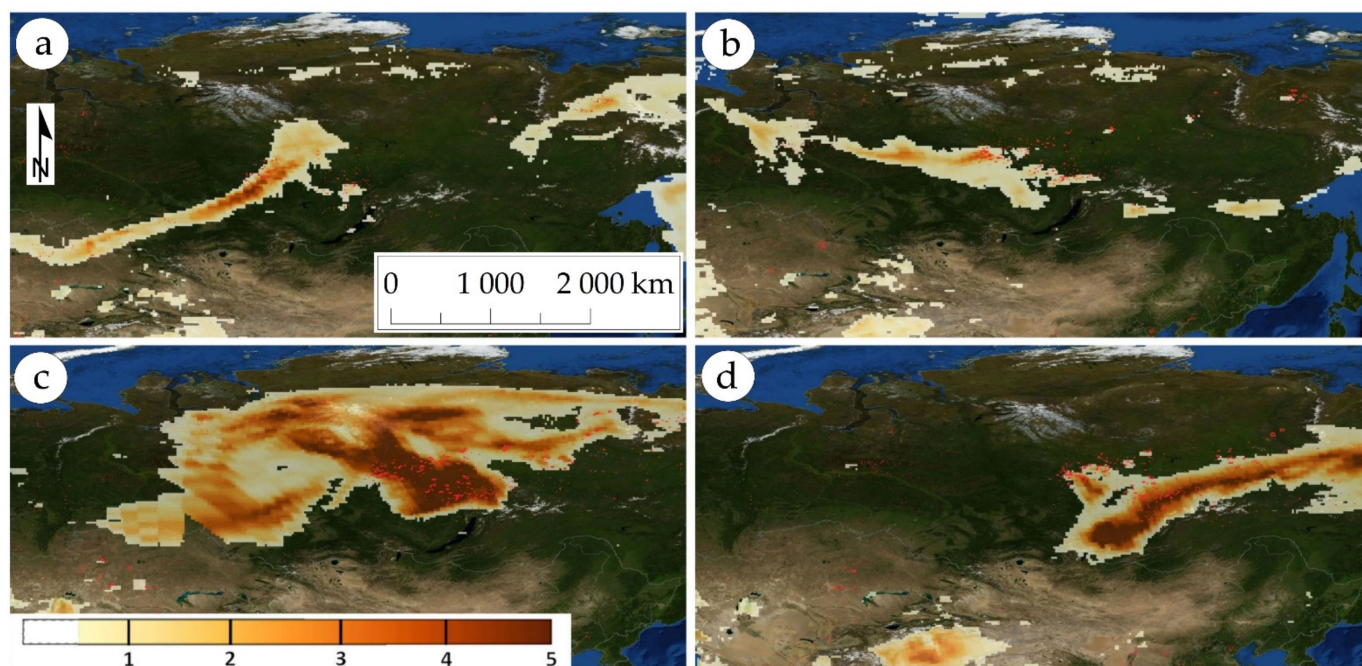


Figure 6. Aerosol Index data for Siberia in the summer of 2019 available from the OMPS Nadir-Mapper instrument on the Suomi National Polar-orbiting Partnership (Suomi NPP) satellite: (a) 14 July; (b) 19 July; (c) 24 July; (d) 29 July.

We can also expect increased fire in deep peats and organic soils in western and northern Siberia as permafrost thaw accelerates and extremes in spring and summer temperatures become more frequent [39]. The World Weather Attribution Organization concluded that the heatwave of spring and summer 2020 would have been extremely unlikely without climate change [40]. It is too early to conclusively determine whether the 2020 fire season will still seem extreme by 2050 or whether it is truly a harbinger of things to come. However, there are many reasons to expect that rapid increases in emissions from Siberian fires are inevitable under a changing climate.

4.3. Limitations

The limitations of our work were as follows.

Remote assessment of the intensity of fires allows classification of active burning areas (fire pixels) and evaluation of the proportions of fire areas with low, medium, and high intensity. However, fire intensity data may have gaps due to the Terra and Aqua/MODIS data interval of 4–6 h between observations.

In addition, some uncertainty in assessing fire intensity is associated with partial blocking of the radiation signal from the fire by crowns of tree stands during surface fires, which is most important for relatively high tree cover. Differences in fire regimes among vegetation types and differences in canopy blocking of spring surface fires between deciduous and evergreen species can add to this problem. Fires in deep organic soils and peats can also have a significant amount of subsurface smoldering, which is not fully observable from satellite observations of FRP. These questions require further research and calibration [49].

Uncertainty is also present in the data on vegetation types and pre-fire fuel loads, which we have summarized from published field data. The vegetation database that we used does not map partly forested peatlands as a separate type, for example, although these are extensive in areas such as western Siberia. We suggest that data on burned areas are more precise at present than resolution and attributive information of available data on vegetation distribution and fuel characteristics for Siberia.

Vegetation models and some field observations suggest that we can expect shifts in vegetation distribution and fuel load over time as climate or management practices

change [47,48]. In this paper, we do not incorporate such potential changes, which would affect fire regimes and emissions.

Our projection of potential fire emissions is an estimate for extreme scenarios. Recalculation of forecast values in relation to fuel loads is a potential for future research.

5. Conclusions

The average annual burned areas for the past 10 years in Siberia were about 2.3 times those for the previous 10 years. This is a strong indication that the warming climate is driving large changes in burned area and carbon emissions and that these increases can be expected to continue in the future. The growth in the number and areas of wildfires in Siberia will determine further increases in carbon emissions. Extrapolation of data for the past two decades suggests a possible ten-fold increase in fire emissions (up to 1500 Tg C/year) by 2050. Fires north of latitude 60°N are likely to contribute the most to emissions growth. Moreover, under conditions of temperature increase and fire activity shifting to the northern regions of Siberia, the contribution to the total emissions from burning in tundra may significantly increase (from <1% of total at present to more than 3%), as occurred in the unusually severe fire year of 2020.

As fires increase in size and intensity, we can also expect that air quality in Siberia in summer will be increasingly affected by growing fire emissions.

Author Contributions: Conceptualization, E.P.; methodology, E.P.; software, N.Y., E.P.; validation, S.G.C., E.P. and T.P.; resources, E.P., O.Y.; data curation, E.P., S.G.C.; writing—original draft preparation, E.P., S.G.C.; writing—review and editing, S.G.C., E.P.; visualization, E.P., N.Y., O.Y.; supervision, E.P.; funding acquisition, O.Y., T.P. All authors have read and agreed to the published version of the manuscript.

Funding: This work was performed using the subject of project no. 0287-2019-0006. This research was partly funded by the Russian Foundation for Basic Research (RFBR) and Government of the Krasnoyarsk krai, and Krasnoyarsk krai Foundation for Research and Development Support, no. 20-44-242002. Grant of Siberian Federal University and Government of the Krasnoyarsk krai, and Krasnoyarsk krai Foundation for Research and Development Support “Long-term consequences of extreme fires in the permafrost zone of Siberia by the materials of satellite monitoring”, 2020, no. KF-782 49/20. The data on wildfires was obtained and initially analyzed in 2004–2013 with the support of the NASA Land Cover Land Use Change (LCLUC) and Terrestrial Ecosystems (TE) programs.

Institutional Review Board Statement: Not applicable.

Informed Consent Statement: Not applicable.

Data Availability Statement: Publicly available datasets were analyzed in this study. This data can be found here: <https://ladsweb.modaps.eosdis.nasa.gov/> (accessed on 25 March 2021), <http://pro-vega.ru/maps/> (accessed on 25 March 2021), and <https://worldview.earthdata.nasa.gov/> (accessed on 13 April 2021).

Acknowledgments: The satellite data-receiving equipment used was provided by the Centre of Collective Usage of Federal Research Center “Krasnoyarsk Science Center, Siberian Branch of Russian Academy of Sciences”, Krasnoyarsk, Russia. Since 2017 we have been monitoring fires as an activity of The Regional Eurasian Fire Monitoring Center (Krasnoyarsk, Russia) under an agreement between V.N. Sukachev Institute of Forest (Krasnoyarsk, Russia) and The Global Fire Monitoring Center (GFMC, Germany, <https://gfmc.online/>). Graphic abstract design by Georgy Ponomarev.

Conflicts of Interest: The authors declare no conflict of interest.

References

1. Conard, S.G.; Sukhinin, A.I.; Stocks, B.J.; Cahoon, D.R.; Davidenko, E.P.; Ivanova, G.A. Determining effects of area burned and fire severity on carbon cycling and emissions in Siberia. *Clim. Chang.* **2002**, *55*, 197–211. [CrossRef]
2. McRae, D.J.; Conard, S.G.; Ivanova, G.A.; Sukhinin, A.I.; Baker, S.; Samsonov, Y.N.; Blake, T.W.; Ivanov, V.A.; Ivanov, A.V.; Churkina, T.V.; et al. Variability of fire behavior, fire effects, and emissions in Scotch pine forests of Central Siberia. *Mitig. Adapt. Strateg. Glob. Chang.* **2006**, *11*, 45–74. [CrossRef]
3. Shvidenko, A.Z.; Schepaschenko, D.G. Climate Change and Wildfires in Russia. *Contemp. Probl. Ecol.* **2013**, *6*, 50–61. [CrossRef]

4. Kharuk, V.I.; Ponomarev, E.I.; Ivanova, G.I.; Dvinskaya, M.L.; Coogan, S.C.P.; Flannigan, M.D. Wildfires in the Siberian taiga. *Ambio* **2021**. [CrossRef]
5. Bondur, V.; Gordo, K.A.; Kladov, V.L. Spacetime Distributions of Wildfire Areas and Emissions of Carbon-Containing Gases and Aerosols in Northern Eurasia according to Satellite-Monitoring Data. *Izv. Atmos. Ocean. Phys.* **2017**, *53*, 859–874. [CrossRef]
6. Ponomarev, E.I.; Shvetsov, E.G.; Kharuk, V.I. The Intensity of Wildfires in Fire Emissions Estimates. *Russ. J. Ecol.* **2018**, *49*, 492–499. [CrossRef]
7. Panov, A.V.; Prokushkin, A.S.; Bryukhanov, A.V.; Korets, M.A.; Ponomarev, E.I.; Sidenko, N.V.; Zrazhevskaya, G.K.; Timokhina, A.V. A Complex Approach for the Estimation of Carbonaceous Emissions from Wildfires in Siberia. *Russ. Meteorol. Hydrol.* **2018**, *43*, 295–301. [CrossRef]
8. NASA. Siberian Smoke Reaches, U.S. and Canada. 2019. Available online: <https://www.nasa.gov/image-feature/goddard/2019/siberian-smoke-reaches-us-canada> (accessed on 25 March 2021).
9. Cottle, P.; Strawbridge, K.; McKendry, I. Long-range transport of Siberian wildfire smoke to British Columbia: Lidar observations and air quality impacts. *Atmos. Environ.* **2014**, *90*, 71–77. [CrossRef]
10. Goldammer, J.G. (Ed.) *Vegetation Fires and Global Change. Challenges for Concerted International Action. A White Paper directed to the United Nations and International Organizations*; Kessel Publishing House: Remagen-Oberwinter, Germany, 2013. Available online: <http://www.fire.unifreiburg.de/latestnews/Vegetation-Fires-GlobalChange-UN-White-Paper-GFMC-2013.pdf> (accessed on 25 March 2021).
11. Soja, A.J.; Cofer, W.R.; Shugart, H.H.; Sukhinin, A.I.; Stackhouse, P.W., Jr.; McRae, D.J.; Conard, S.G. Estimating fire emissions and disparities in boreal Siberia (1998–2002). *J. Geophys. Res.* **2004**, *109*, D14S06. [CrossRef]
12. Ivanova, G.A.; Ivanov, V.A.; Kukavskaya, E.A.; Conard, S.G.; McRae, D.J. Effect of Fires on Carbon Emission in the Pine Forests of Middle Siberia. *Sib. J. Ecol.* **2007**, *14*, 885–895. (In Russian)
13. Conard, S.G.; Ivanova, G.A. Wildfire in Russian Boreal Forests—Potential Impacts of Fire Regime Characteristics on Emissions and Global Carbon Balance Estimates. *Environ. Pollut.* **1997**, *98*, 305–313. [CrossRef]
14. Kukavskaya, E.; Soja, A.; Petkov, A.; Ponomarev, E.; Ivanova, G.; Conard, S. Fire Emissions Estimates in Siberia: Evaluation of Uncertainties in Area Burned, Land Cover, and Fuel Consumption. *Can. J. For. Res.* **2013**, *43*, 493–506. [CrossRef]
15. Bartalev, S.A.; Stytsenko, F.V.; Egorov, V.A.; Loupian, E.A. Satellite assessment of fire-caused forest mortality in Russia. *Forestry (Lesovedenie)* **2015**, *2*, 83–94. (In Russian)
16. Wooster, M.J.; Roberts, G.; Perry, G.L.W.; Kaufman, Y.J. Retrieval of biomass combustion rates and totals from fire radiative power observations: FRP derivation and calibration relationships between biomass consumption and fire radiative energy release. *J. Geophys. Res.* **2005**, *110*, D24311. [CrossRef]
17. Ichoku, C.; Kaufman, Y.J. A method to derive smoke emission rates from MODIS fire radiative energy measurements. *IEEE Trans. Geosci. Remote Sens.* **2005**, *43*, 2636–2649. [CrossRef]
18. Vermote, E.; Ellicott, E.; Dubovik, O.; Lapyonok, T.; Chin, M.; Giglio, L.; Roberts, G.J. An approach to estimate global biomass burning emissions of organic and black carbon from MODIS fire radiative power. *J. Geophys. Res.* **2009**, *114*, 1–22. [CrossRef]
19. Shvidenko, A.Z.; Shchepashchenko, D.G.; Vaganov, E.A.; Sukhinin, A.I.; Maksyutov, S.; McCallum, I.; Lakyda, I.P. Impact of wildfire in Russia between 1998–2010 on ecosystems and the global carbon budget. *Dokl. Earth Sci.* **2011**, *441*, 1678–1682. [CrossRef]
20. Zamolodchikov, D.G.; Grabovskii, V.I.; Kraev, G.N. Dynamics of Carbon Budget in Forests of Russia for Last Twenty Years. *Forestry* **2011**, *6*, 16–28. (In Russian)
21. Balashov, I.; Bartalev, S.; Burtsev, M.; Vorushilov, I.; Egorov, V.; Kashnitskii, A.; Khovratovich, T.; Khvostikov, S.A.; Kobets, D.; Loupian, E.; et al. Vega-Les Information System. Actual Features and Future Evolution. *IOP Conf. Ser. Earth Environ. Sci.* **2020**, *507*, 012002. [CrossRef]
22. Ponomarev, E.I.; Shvetsov, E.G. Satellite detection of forest fires and geoinformation methods for calibrating of the result. *Issled. Zemli Kosm. (Remote Sens.)* **2015**, *1*, 84–91. (In Russian) [CrossRef]
23. Giglio, L.; Descloitres, J.; Justice, C.; Kaufman, Y. An enhanced contextual fire detection algorithm for MODIS. *Remote Sens. Environ.* **2003**, *87*, 273–282. [CrossRef]
24. Ponomarev, E.I.; Shvetsov, E.G.; Litvintsev, K.Y. Calibration of Estimates on Direct Wildfire Emissions from Remote Sensing Data. *Izv. Atmos. Ocean. Phys.* **2019**, *55*, 1065–1072. [CrossRef]
25. Seiler, W.; Crutzen, P.J. Estimates of gross and net fluxes of carbon between the biosphere and atmosphere from biomass burning. *Clim. Change* **1980**, *2*, 207–247. [CrossRef]
26. Ivanova, G.A.; Kukavskaya, E.A.; Ivanov, V.A.; Conard, S.G.; McRae, D.J. Fuel characteristics, loads and consumption in Scots pine forests of central Siberia. *J. For. Res.* **2020**, *31*, 2507–2524. [CrossRef]
27. Tsvetkov, P.A. Adaptation of *Larix gmelinii* to Fires in the Northern Taiga of Central Siberia. *Sib. J. Ecol.* **2005**, *1*, 117–129. (In Russian)
28. De Groot, W.J.; Cantin, A.S.; Flannigan, M.D.; Soja, A.J.; Gowman, L.M.; Newbery, A. A comparison of Canadian and Russian boreal forest fire regimes. *For. Ecol. Manag.* **2013**, *294*, 23–34. [CrossRef]
29. Shvetsov, E.G.; Ponomarev, E.I. Postfire Effects in Siberian Larch Stands on Multispectral Satellite Data. *Contemp. Probl. Ecol.* **2020**, *13*, 104–112. [CrossRef]

30. IPCC. *Climate Change 2014: Impacts, Adaptation, and Vulnerability; Summaries, Frequently Asked Questions, and Cross-Chapter Boxes*, Report of the Intergovernmental Panel on Climate Change; Field, C.B., Barros, V., Dokken, D.J., Mach, M.D., Mastrandrea, T.E., Bilir, M., Eds.; World Meteorological Organization: Geneva, Switzerland, 2014.
31. Valendik, E.N.; Kisilyakhov, E.K.; Ryzhkova, V.A.; Ponomarev, E.I.; Danilova, I.V. Conflagration fires in taiga landscapes of Central Siberia. *Geogr. Nat. Resour.* **2014**, *35*, 41–47. [[CrossRef](#)]
32. Hayasaka, H.; Yamazaki, K.; Naito, D. Weather conditions and warm air masses during active fire-periods in boreal forests. *Polar Sci.* **2019**, *22*, 100472. [[CrossRef](#)]
33. Conard, S.G.; Ponomarev, E.I. Fire in the North—The 2020 Siberian Fire Season. *Wildfire* **2020**, *29*, 26–32.
34. Witze, A. The Arctic is burning like never before—And that’s bad news for climate change. *Nature* **2020**, *585*, 336–337. [[CrossRef](#)] [[PubMed](#)]
35. Amiro, B.; Cantin, A.; Flannigan, M.; De Groot, W. Future Emissions from Canadian boreal forest fires. *Can. J. For. Res.* **2009**, *39*, 383–395. [[CrossRef](#)]
36. Ponomarev, E.I.; Shvetsov, E.G.; Usataya, Y.O. Determination of the Energy Properties of Wildfires in Siberia by Remote Sensing. *Izv. Atmos. Ocean. Phys.* **2018**, *54*, 979–985. [[CrossRef](#)]
37. Ponomarev, E.I.; Kharuk, V.I. Wildfire Occurrence in Forests of the Altai–Sayan Region under Current Climate Changes. *Contemp. Probl. Ecol.* **2016**, *9*, 29–36. [[CrossRef](#)]
38. Ponomarev, E.I.; Skorobogatova, A.S.; Ponomareva, T.V. Wildfire Occurrence in Siberia and Seasonal Variations in Heat and Moisture Supply. *Russ. Meteorol. Hydrol.* **2018**, *43*, 456–463. [[CrossRef](#)]
39. McCarty, J.L.; Smith, T.E.L.; Turetsky, M.R. Arctic fires re-emerging. *Nat. Geosci.* **2020**, *13*, 658–660. [[CrossRef](#)]
40. Ciavarella, A.; Cotterill, D.; Stott, P.; Kew, S.; Sjoukje, P.; Van Oldenborgh, G.J.; Skålevåg, A.; Lorenz, P.; Robin, Y.; Otto, F.; et al. Prolonged Siberian Heat of 2020. World Weather Attribution Organization. 2020. Available online: <https://www.worldweatherattribution.org/siberian-heatwave-of-2020-almost-impossible-without-climate-change> (accessed on 25 March 2021).
41. Wiedinmyer, C.; Neff, J.C. Estimates of CO₂ from fires in the United States: Implications for carbon management. *Carbon Balance Manag.* **2007**, *2*. [[CrossRef](#)]
42. Veraverbeke, S.; Rogers, B.M.; Randerson, J.T. Daily burned area and carbon emissions from boreal fires in Alaska. *Biogeosciences* **2015**, *12*, 3579–3601. [[CrossRef](#)]
43. Amiro, B.D.; Todd, J.B.; Wotton, B.M.; Logan, K.A.; Flannigan, M.D.; Stocks, B.J.; Mason, J.A.; Martell, D.L.; Hirsch, K.G. Direct carbon emissions from Canadian forest fires, 1959 to 1999. *Can. J. For. Res.* **2001**, *31*, 512–525. [[CrossRef](#)]
44. Chen, G.; Hayes, D.J.; David McGuire, A. Contributions of wildland fire to terrestrial ecosystem carbon dynamics in North America from 1990 to 2012. *Glob. Biogeochem. Cycles* **2017**, *31*, 878–900. [[CrossRef](#)]
45. Torres, O.; Bhartia, P.K.; Herman, J.R.; Ahmad, Z.; Gleason, J. Derivation of aerosol properties from satellite measurements of backscattered ultraviolet radiation: Theoretical basis. *J. Geophys. Res.* **1998**, *103*, 17099–17110. [[CrossRef](#)]
46. Ponomarev, E.I.; Kharuk, V.I.; Ranson, J.K. Wildfires Dynamics in Siberian Larch Forests. *Forests* **2016**, *7*, 125. [[CrossRef](#)]
47. Tchebakova, N.M.; Parfenova, E.I.; Soja, A.J. Significant Siberian Vegetation Change is Inevitably Brought on by the Changing Climate. In *Novel Methods for Monitoring and Managing Land and Water Resources in Siberia*; Mueller, L., Sheudshen, A., Eulenstein, F., Eds.; Springer Water, Springer: Cham, Switzerland, 2016; pp. 269–285. [[CrossRef](#)]
48. Kukavskaya, E.A.; Buryak, L.V.; Shvetsov, E.G.; Conard, S.G.; Kalenskaya, O.P. The impact of increasing fire frequency on forest transformations in southern Siberia. *For. Ecol. Manag.* **2016**, *382*, 225–235. [[CrossRef](#)]
49. Mathews, B.J.; Strand, E.K.; Smith, A.M.; Hudak, A.T.; Dickinson, B.; Kremens, R.L. Laboratory experiments to estimate interception of infrared radiation by tree canopies. *Int. J. Wildland Fire* **2016**, *25*, 1009–1014. [[CrossRef](#)]